



# Journal of Thailand Concrete Association

## วารสารวิชาการสมาคมคอนกรีตแห่งประเทศไทย

### A SIMPLIFIED MODEL FOR PREDICTION OF SHRINKAGE BEHAVIOUR OF HIGH PERFORMANCE CONCRETE CONTAINING SUPPLEMENTARY CEMENTITIOUS MATERIALS

Qizhe Hou<sup>1</sup> Kejin Wang<sup>2\*</sup> Wanchai Yodsudjai<sup>3</sup>

<sup>1</sup> Department of Civil and Environmental Engineering, Iowa State University, Ames, IA, USA

<sup>2</sup> Department of Civil and Environmental Engineering, Iowa State University, Ames, IA, USA

<sup>3</sup> Department of Civil Engineering, Faculty of Engineering, Kasetsart University, Bangkok, Thailand

#### ARTICLE INFO:

*Received: February 16, 2016*

*Received Revised Form:*

*June 17, 2016*

*Accepted: July 1, 2016*

#### ABSTRACT :

In this study, autogenous and drying shrinkage of nine high performance concrete (HPC) mixes that are commonly used for bridge decks and bridge overlays were monitored with time. The mixes contained 10-30% of class C fly ash (FA) and 25-45% ground granulated blast-furnace slag (GGBFS) replacement for cement. Based on the shrinkage measurements, a statistical model was developed for describing and predicting shrinkage behaviour of concrete made with different types and amounts of supplementary cementitious materials (SCMs). The results indicate that this new simplified, exponential model can well predict shrinkage behavior of concrete and mortar made with materials similar to those used in the present study. From the newly developed model, the physical meaning of ultimate shrinkage and rate of shrinkage are further elucidated, and the effects of SCMs on concrete shrinkage behaviour are clearly expounded.

*\*Corresponding Author,  
Email address: kejinw@iastate.edu*

**KEYWORDS:** shrinkage, model, fly ash, slag, high performance concrete

#### 1. Introduction

High-performance concrete (HPC) is widely used for construction of bridge decks and overlays because of its rapid strength development, low permeability, and excellent durability. However, due to its high paste content, low water-to-binder ratio (w/b), and high dosage of chemical admixtures, HPC often displays considerably higher autogenous shrinkage than normal strength concrete (NSC), resulting in a significant contribution to the total shrinkage of the concrete.

Due to the environmental, functional, and economic considerations, supplementary cementitious materials (SCMs), such as fly ash (FA) and ground granulated blast-furnace slag (GGBFS), are becoming necessary constituents in concrete. Researches have shown that fly ash replacement for cement generally reduces both autogenous shrinkage

[1] and drying shrinkage [2] of concrete. However, GGBFS replacement for cement often leads to different effects on autogenous shrinkage drying shrinkage of concrete, depending up on the chemical and physical properties of the slag. As a result, the effect of GGBFS replacement on the total shrinkage of concrete is often inconsistent [3,4].

Many models have been proposed for predicting concrete shrinkage behavior. Some numerical models are often complicated due to the involvements of many factors, such as concrete surface-to-volume ratio, cementitious material type and content, water-to-cement ratio, aggregate content, admixtures, and environmental conditions [5], while other empirical models, such as ACI 209R-92, B3, CEB MC90, CEB MC90-99, and GL2000 models, often fit concrete mixes with little or no SCMs and chemical admixtures [6].

In the present study, a set HPC mixes made with different amounts of fly ash and GGBFS replacement for cement was studied, and the shrinkage behavior of these concrete mixes was characterized. A statistical analysis conducted to develop a simple model to predict autogenous and drying shrinkage of HPC with commonly used SCMs and admixtures.

## 2. Materials and mix proportions

Type I/II and IP cement, Class C fly ash, and ground granulated blast furnace slag (GGBFS) that meet ASTM C150, C618 and C989, respectively, were used. The chemical and physical properties of these cementitious materials are presented in Table 1.

The fine aggregate used was river sand with specific gravity of 2.64, absorption of 1.4%, and fineness modulus of 3.13. Nine mix proportions of mortars, as presented in Table 2, were selected from the HPC mixes that are commonly used for bridge decks and overlays in Iowa, USA. The mixes had different cement and sand content and different type and dosage of chemical admixtures. During the data analysis, the test results from the first seven mixes in Table 2 were used for the shrinkage model development, while the last two mixes (Mixes PC' and 20F') were designed, as independent samples, for the validation of the newly-developed shrinkage model.

**Table 1** Properties of cementitious materials

Type	Chemical composition (%)									Fineness
	CaO	Al <sub>2</sub> O <sub>3</sub>	SiO <sub>2</sub>	Fe <sub>2</sub> O <sub>3</sub>	SO <sub>3</sub>	MgO	Na <sub>2</sub> O	K <sub>2</sub> O	LOI	(m <sup>2</sup> /kg)
I/II	63.1	4.6	20.2	3.2	3.4	2.4	0.09	0.67	1.2	397
IP	48.3	8.9	29.3	4.1	3.1	3.1	0.30	0.70	1.7	490
FA	23.7	22.0	37.3	6.3	1.6	5.3	1.16(Na <sub>2</sub> O) <sub>eq</sub>		0.25	15.8%*
GGBFS	37.1	9.2	36.8	0.76	-	9.5	0.34	0.41	-	534

\* Fineness of the fly ash expressed as the percentage passing the 45- $\mu$ m (No. 325) sieve.

**Table 2.** Mix properties of mortar (per cubic meter)

ID	Cement type I/II	Fly Ash (slag)	Sand	s/b	Water	w/b	AEA	MRWR (NRWR)	Retarder
	kg	kg	kg		kg		ml	ml	ml
1-PC	421	-	834	1.98	169	0.4	378	1259	419
2-25S	316	(105)	834	1.98	169	0.4	378	1259	419
3-35S	274	(147)	834	1.98	169	0.4	378	1259	419
4-45S	232	(189)	834	1.98	169	0.4	378	1259	419
5-10F	379	42	834	1.98	169	0.4	378	1259	419
6-20F	337	84	834	1.98	169	0.4	378	1259	419
7-30F	295	127	834	1.98	169	0.4	378	1259	419
8-PC'*	396	-	835	2.11	159	0.4	354	(708)	394
9-20F'*	273	68	883	2.59	143	0.42	378	(610)	348

\* Mixes with Type IP cement

## 3. Experimental work

Autogenous and drying shrinkage of all nine HPC mortar mixes in Table 2 were monitored with time. The tests were performed under the standard environmental conditions as described in ASTM

C596 and ACI 209.2R-08. The detailed information on the tests is provided as below.

### 3.1 Set time test

According to ASTM C 1698, the first measurement of the autogenous shrinkage of a tested mortar shall be at the exact moment of the final set time

of the mortar. Therefore, set time tests were performed for all the 9 mixes studied according to ASTM C403/C403M.

### 3.2 Autogenous shrinkage test

Autogenous shrinkage tests of mortars were performed according to ASTM C 1698 [7]. For each mortar mix, materials were first mechanically mixed according to ASTM C305. Three samples were then cast in 30 mm (diameter)  $\times$  300 mm (length) corrugated polyethylene tubes/molds (Figure 1a). The samples were consolidated with a vibration table with amplitude of 3,600 VPM for 15 to 30 seconds. After the ends were properly sealed, the samples were then placed horizontally on a smooth surface to avoid any unexpected length change due to its gravity and kept in an environmental chamber with an ambient temperature of  $23\pm1^\circ\text{C}$  (Figure 1b).

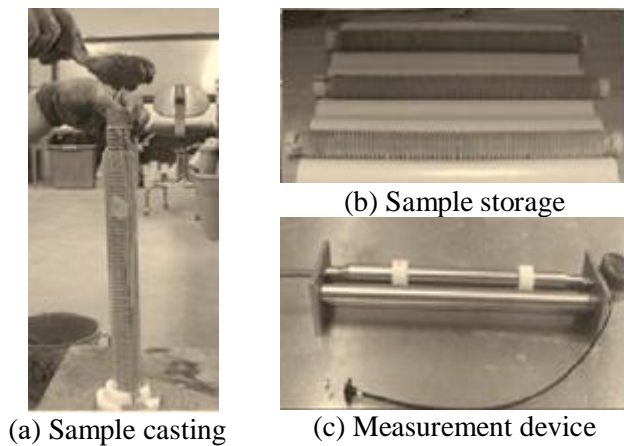


**Figure 1** Sample preparation for autogenous shrinkage tests

To minimize test errors, the length measurement device was also kept in the same environmental chamber where the samples were stored (Figure 1c). The length measurements of the free drying shrinkage mortar samples were then taken at 1, 3, 7 days and then once a week up to 56 days.

### 3.3 Autogenous shrinkage test

Drying shrinkage tests were performed for all 9 mortar mixes studied according to ASTM C 596 [8]. For each mortar mix, three prism samples ( $25 \times 25 \times 285$  mm, Figure 2a) were made from the same batch used for preparation of the corresponding autogenous shrinkage test samples. Vibration table was also applied for consolidation. The samples used for drying shrinkage tests were first cured in a moist room ( $23\pm1^\circ\text{C}$  and 100% RH) for 1 day and then placed in a lime-saturated water tank at  $23\pm1^\circ\text{C}$  for 2 days. At the age of  $72\pm0.5$  hours, the samples were

removed from the water tank and measured for their initial length immediately. They were then placed in the environment room with  $23\pm1^\circ\text{C}$  and 40% RH for drying (Figure 2b). The length measurements of the drying shrinkage mortar samples were then taken at 1, 3, 7 days and then once a week up to 56 days (Figure 2c).

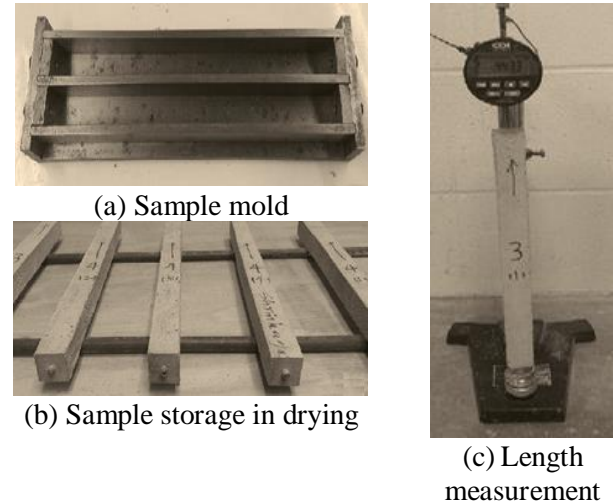


**Figure 2** Test device and specimens of drying shrinkage of mortar

## 4. Experimental Results

### 4.1 Set time of mortars

Figure 3 shows the set times of all mortar mixes studied. It is observed from the figure that the initial and final set times were delayed up to 2 hours for the mortar made with GGBFS replacement level of 45%, and they were postponed by approximate 4 hours for the mortar made with 30% FA replacement.

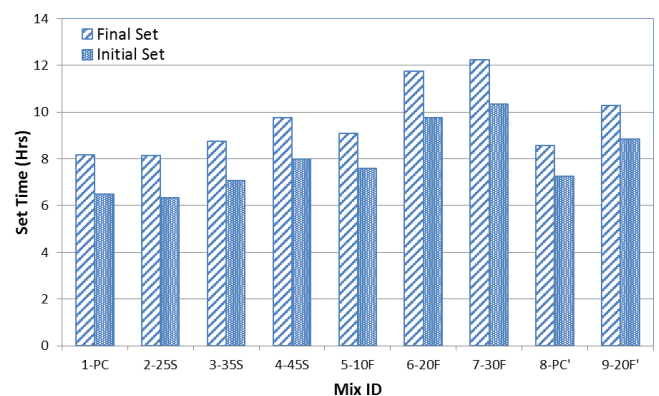
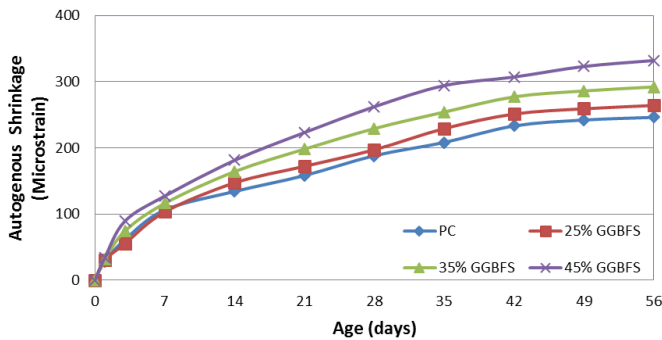


**Figure 3** Initial and final set time of mortars

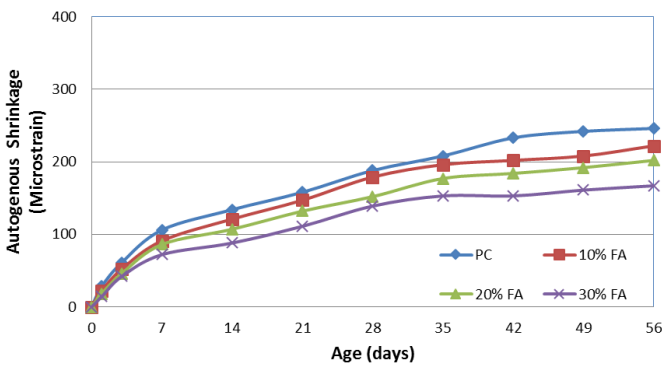
As mentioned previously, final set times measured were used as the time for taking the initial autogenous shrinkage measurements.

#### 4.2 Autogenous shrinkage

Figure 4 shows that the effects of SCMs on autogenous shrinkage vary depending on the type and amount of the SCM replacement in mixes.



(a) Effect of GGBFS



(b) Effect of fly ash

**Figure 4** Effect of slag and fly ash replacement on autogenous shrinkage of mortar

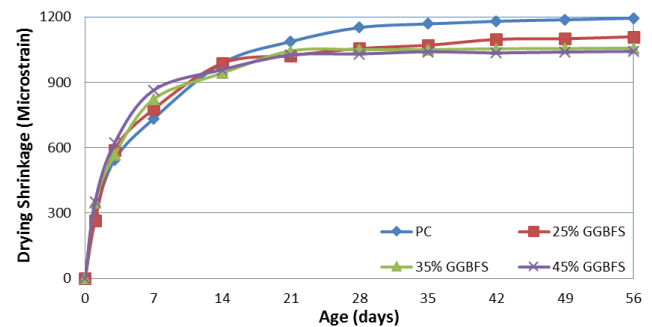
As shown in Figure 4(a), increased GGBFS replacement level led to an increase in autogenous shrinkage of a mortar. This may be attributed to the higher paste volume of the GGBFS mixes, resulting from the lower specific gravity of the GGBFS than that of Portland cement, and refined pores in the pastes. [9]

On the other hand, as shown in Figure 4(b), increased fly ash (FA) replacement caused an increased reduction in autogenous shrinkage. As the FA replacement level increased up to 30%, the ultimate autogenous shrinkage was reduced about 22%. This was agreed with the study result of Tangtermsirikul [10] which was found that FA was effective for reducing both autogeneous and drying shrinkages. One of the shrinkage reduction mechanisms provided by fly ash in concrete is the reduction of water demand in fly ash concrete. Having smooth particle surface and spherical particle shape, fly ash increases “effective” mixing water in

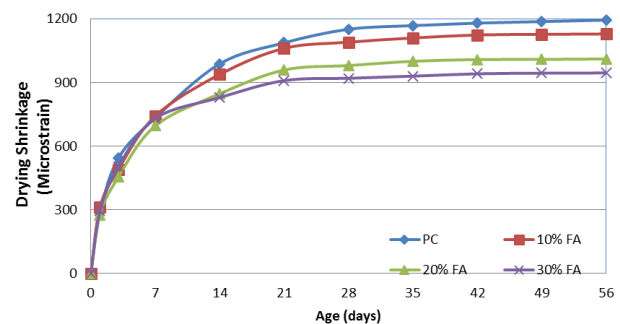
concrete [11] at a given water-to-cementitious material ratio (w/cm). As more free water exists inside concrete, less self-desiccation will occur and all water loss related shrinkages (both autogenous and drying shrinkages) of the concrete are generally reduced [12].

#### 4.3 Drying shrinkage

Figure 5 illustrates the effects of SCMs on drying shrinkage of the mortars studied. As seen in Figure 6a, GGBFS replacement increased drying shrinkage during the first seven days of drying. The higher the GGBFS replacement level was the higher the drying shrinkage value of the mortar at the early age. However, after seven days, GGBFS replacement noticeably reduced drying shrinkage of the mortar. The higher the GGBFS replacement level, the higher the drying shrinkage reduction the mortar has at later ages [13]. It is possible that after several days of drying, the pozzolanic reaction of GGBFS enhanced the strength of the mortar and improved the deformation resistance [3].



(a) Effect of GGBFS



(b) Effect of fly ash

**Figure 5** Effect of slag and fly ash replacement on drying shrinkage of mortar

Different from GGBFS replacement, Figure 5(b) shows that fly ash replacement clearly reduced drying shrinkage of the mortar. The reduction is more significant at later ages. As mentioned previously, the

reduction in drying shrinkage may be due to the reduced water demand of fly ash mortar or concrete [10].

It shall be noted that at the early age (7 or 14 days) of testing, the rates of both autogenous shrinkage and drying shrinkage are high, as indicated by the slopes of the curves in Figures 4 and 5. After 14 days, the rates of autogenous shrinkage of the tested mortars appeared reduced slightly but were still very high, while the rates of drying shrinkage of the corresponding mortars were significantly reduced, evidenced by the plateaus. The high rates of autogenous shrinkage of the tested mortars at the later age may be contributed by the long-term self-desiccation in the HPC mortar, while the significantly reduced rates of drying shrinkage of the mortar at the later age may result from the improved microstructure and strength development of the mortar with time, which enhances deformation resistance of the mortar.

## 5. Experimental Results

### 5.1 Model development

Based on the present experimental results, an exponential 3P model can be established for predicting autogenous shrinkage and drying shrinkage using a statistical method. Figure 6 shows a typical exponential 3P fitting model developed from the autogenous shrinkage test data of mortar Mix 5-10F (with 10% fly ash replacement) and analyzed by statistic computer software JMP® [14].

Such an exponential model is actually applicable for all autogenous and drying shrinkage measurements obtained from the present study. Therefore, a general form of the autogenous and drying shrinkage model is selected as described in Equation 1.

$$\varepsilon(t) = a + b \cdot e^{(c \cdot t)} \quad (\text{Eq. 1})$$

where  $\varepsilon(t)$  is either autogenous shrinkage  $\varepsilon_{\text{auto}}(t)$  or drying shrinkage  $\varepsilon_{\text{drying}}(t)$  (microstrain) of the mortar at the corresponding age of  $t$ ;  $a$  (Asymptote),  $b$  (Scale), and  $c$  (Growth Rate) are model parameters;  $t$  is the testing age of mortar ( $\leq 56$  days). Table 3 presents the 3P fitting model parameters obtained from JMP® for autogenous and drying shrinkage of the seven mortar mixes studied.

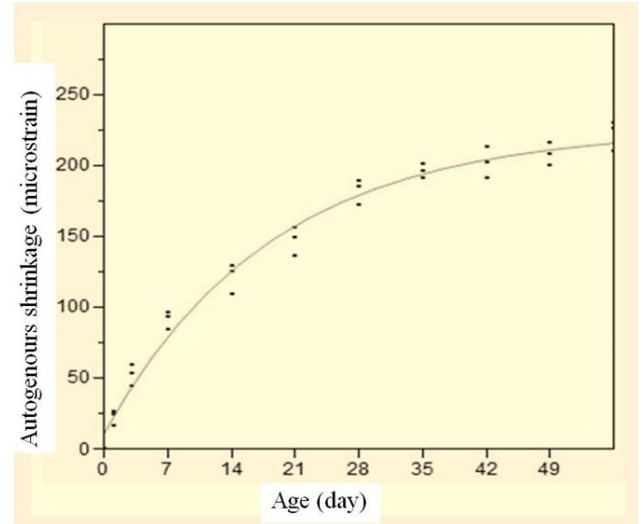


**Figure 6** Typical curve fitting for autogenous shrinkage of mix with 10% fly ash

As shown, scale (b) is used associated with asymptote (a) to indicate the ultimate shrinkage of a given mix. In addition, growth rate (c) indicates the speed of shrinkage from initial to ultimate state. Generally, a greater absolute value of growth rate (c) results in a shorter time to reach the ultimate shrinkage; or the faster shrinkage speed. As seen in Table 3, the parameters,  $a$  (asymptote),  $b$  (scale), and  $c$  (growth rate), varied with the type and replacement level of SCMs, except that the growth rates ( $c$ ) of autogenous shrinkage were kept as  $-0.05$  for six out of seven mortar mixes studied. Since the growth rates are all negative, the term  $b \cdot e^{(c \cdot t)}$  gets close to 0 as age ( $t$ ) approaches the ultimate testing date (56 days in the present study). Therefore, the asymptote ( $a$ ) actually represents the ultimate shrinkage value ( $\varepsilon_{\text{ult}}$ ). That is:

$$a \approx \varepsilon_{\text{ult}} \quad (\text{for both autogenous and drying shrinkages}) \quad (\text{Eq. 2})$$

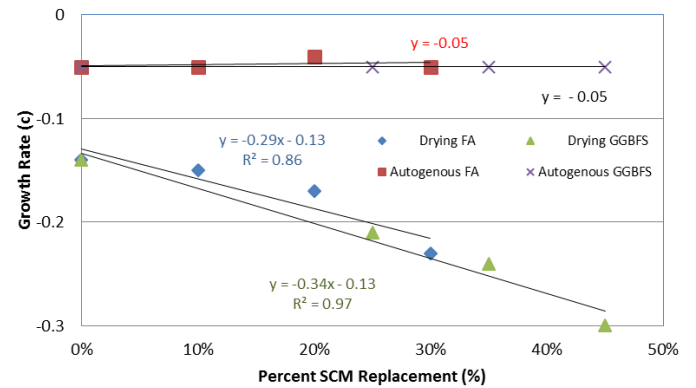
Based on Equation 1, the absolute values of scale  $|b|$  shall be equal to the value of asymptote  $a$ . Thus, shrinkage value  $\varepsilon$  will be zero when the testing time  $t$  is zero, i. e.,  $\varepsilon(0) = 0$ . Table 3 shows that there are small differences between asymptote values ( $a$ ) and their corresponding absolute scale values  $|b|$ , which are probably caused by the 3P curve fitting of the test data.



**Table 3** Regression coefficients for modeling shrinkage of mortar

Shrinkage Type	Model Parameter	PC (Control)	10% FA	20% FA	30% FA	25% Slag	35% Slag	45% Slag
Autogeneous	Asymptote (a)	262	226	222	202	280	290	322
	Scale (b)	-245	-215	-209	-192	-266	-275	-305
	Growth Rate (c)	-0.05	-0.05	-0.04	-0.05	-0.05	-0.05	-0.05
Drying	Asymptote (a)	1171	1113	996	924	1072	1042	1024
	Scale (b)	-1090	-1037	-935	-876	-1031	-984	-986
	Growth Rate (c)	-0.14	-0.15	-0.17	-0.23	-0.21	-0.24	-0.30

Figure 7 shows that there are linear relationships between each of the model parameters and SCM replacement level for a given mortar mix. Figure 7a confirms that the ultimate dry shrinkage values decreased with GGBFS and fly ash replacements for cement; while the ultimate autogeneous shrinkage values decreased with fly ash replacement but increased with GGBFS replacement. Inversely, Figure 7b elucidates that the scale b values of drying shrinkage increased with GGBFS and fly ash replacements for cement; while the scale b values of autogeneous shrinkage increased slightly with fly ash replacement but decreased slightly with GGBFS replacement.

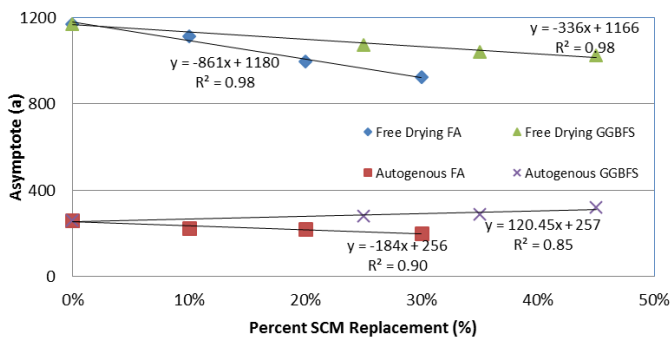


(c) Percent SCM replacement vs. growth rate

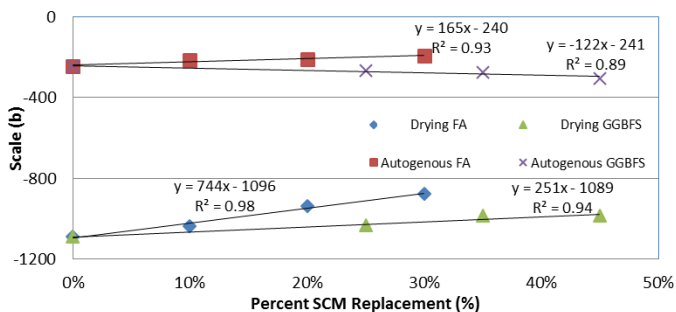
**Figure 7** Relationship between shrinkage model parameters and SCM replacement levels

Figure 7c clarifies that the growth rate (c) can be selected as -0.05 for the autogeneous shrinkage of mortars with and without SCMs (GGBFS or fly ash), while the growth rate (c) of drying shrinkage decreased rapidly with increased GGBFS and fly ash replacements. It is noted from the figure that the slope of the curve of mortar mixes with GGBFS replacement is slightly lower (more negative) than that of mortar mixes with fly ash replacement. Regardless this small difference between GGBFS and fly ash mixes, a linear line as indicated in Equation 3 can fit the growth rates of all the 7 mortar mixes studied quite well. Thus, the growth rates of the mortars can be expressed as:

$$\text{Growth rate (c)} = \begin{cases} -0.05 & \text{(Eq. 3)} \\ \text{(for autogeneous shrinkage)} \\ -0.35(\% \text{SCM}) - 0.21 & \\ (R^2 = 0.91) & \\ \text{(for drying shrinkage)} \end{cases}$$



(a) Percent SCM replacement vs. asymptote



(b) Percent SCM replacement vs. scale

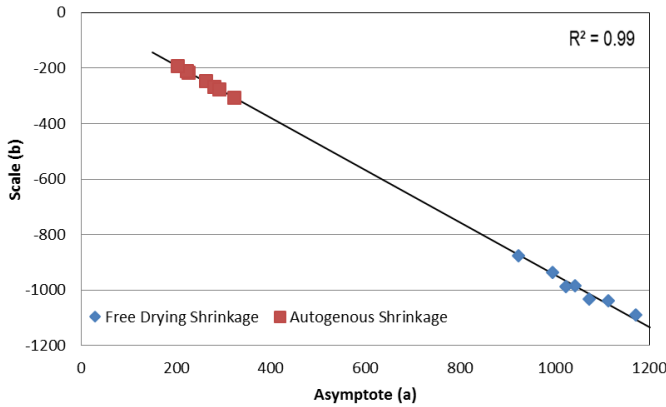
### 5.2 Model development

Figure 8 demonstrates a close linear relationship between the asymptote (a) and scale (b), which can be expressed by Equation 4:

$$b = -0.95 \cdot a \quad (R^2 = 0.99) \quad (\text{Eq. 4})$$

Plugging Equations 2 and 4 into Equation 1, one can obtain Equation 5:

$$\varepsilon(t) = \varepsilon_{ult} [1 - 0.95 \cdot e^{(c-t)}] \quad (\text{Eq. 5})$$



**Figure 8** Relationships between the model coefficients asymptote and scale

$$NS = \begin{cases} -0.72 (\%FA) + 0.99 & \text{(for autogenous and drying shrinkage)} \\ 1.41 (\%GGBSF)^2 - 0.069 (\%GGBFS) + 1.00 & \text{(for autogenous shrinkage)} \\ -0.295 (\%GGBFS) + 1.00 & \text{(for drying shrinkage)} \end{cases} \quad (\text{Eq. 7})$$

Table 4 presents the comparison of measured and predicted ultimate shrinkages of the mortars studied, the latter of which were calculated using Equation 1, together with the parameters listed in Table 3.

To use Equation 5 for shrinkage prediction of mortar or concrete,  $\varepsilon_{ult}$  or asymptote (a) must be known. Since most existing models can predict  $\varepsilon_{ult}$  of concrete without SCMs ( $\varepsilon_{ult, control}$ ), a term, normalized ultimate shrinkage (NS), is introduced to express  $\varepsilon_{ult}$  of concrete with SCMs ( $\varepsilon_{ult, scm}$ ) with  $\varepsilon_{ult, control}$ , as defined in Equation 6:

$$NS = \frac{\varepsilon_{ult, scm}}{\varepsilon_{ult, control}} \quad (\text{for both autogenous and drying shrinkages}) \quad (\text{Eq. 6})$$

Where,  $\varepsilon_{ult, scm}$  and  $\varepsilon_{ult, control}$  are the ultimate shrinkage ( $\varepsilon_{ult}$ ) values of mortar/concrete with and without SCMs, respectively. Similar to Figure 7a, Figure 9 shows that the NS values are closely related to the SCM replacement level. Since NS values for autogenous and drying shrinkages of mortars with fly ash are very close, a linear line as indicated in Equation 7 can fit the data points of all NS values of both autogenous and drying shrinkages of mortars. That is:

**Table 4** Ultimate shrinkage of mortars

Ultimate Shrinkage $\varepsilon_{ult}$ (microstrain)		PC (Control)	10% FA	20% FA	30% FA	25% Slag	35% Slag	45% Slag
Drying $\varepsilon_{ult, drying}$	Measured	1194	1129	1011	945	1109	1057	1042
	Predicted	1171	1113	996	924	1072	1042	1024
Autogenous $\varepsilon_{ult, auto}$	Measured	246	222	212	192	264	282	309
	Predicted	247	213	200	190	264	273	304

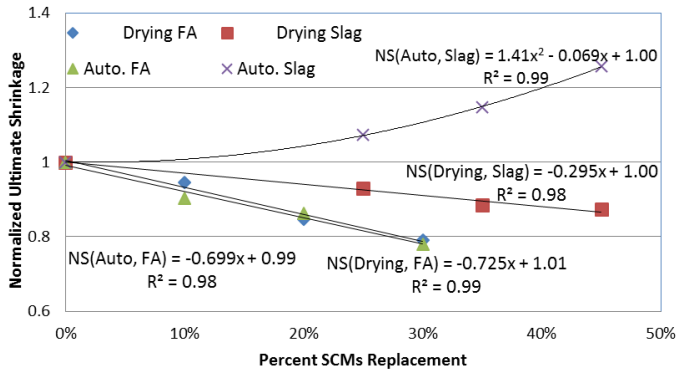


**Figure 9** Relationship between normalized ultimate shrinkage and SCMs replacement level

Using the NS value,  $\varepsilon_{ult,scm} = NS \bullet \varepsilon_{ult,control}$ . Thus, the shrinkage prediction Equation 5 can be rewritten as follows (Equation 8) for mortar or concrete with SCM replacement:

$$\varepsilon_{scm}(t) = NS \bullet \varepsilon_{ult,control} \bullet [1 - 0.95e^{(c \bullet t)}] \quad (\text{Eq. 8})$$

where,  $\varepsilon_{scm}(t)$  is autogenous or drying shrinkage of mortar or concrete with a SCM at testing age of  $t$ ;  $\varepsilon_{ult,control}$  is the ultimate autogenous or ultimate drying shrinkage of mortar or concrete without SCM. For a specific mix, the normalized ultimate shrinkage (NS) and the growth rate ( $c$ ) can be calculated based on Equations 7 and 3, respectively.

### 5.3 Hardened properties of sprayed mortar

Using Equation 8, the autogenous or drying shrinkage of mortar or concrete with a SCM (GGBFS or fly ash) at any testing age can be predicted as long as the ultimate autogenous or ultimate drying shrinkage of mortar or concrete without SCM is known. According to the ACI 209R-92 model, the shrinkage behavior of a basic concrete mix (without SCM) can be predicted from Equation 9, which requires information only on concrete age, curing method, relative humidity, volume to surface ratio, cement type and mix proportion [ผิดพลาด! ไม่ได้กำหนดที่ต้นหน้า].

$$E_{sh}(t, t_c) = \frac{t - t_c}{f + (t - t_c)} \bullet \varepsilon_{shu} \quad (\text{Eq. 9})$$

**Table 5** Model adjustment factors for ACI 209R-92 [ผิดพลาด! ไม่ได้กำหนดที่ต้นหน้า]

Coefficients	$\gamma_{sh,tc}$	$\gamma_{sh,RH}$	$\gamma_{sh,vs}$	$\gamma_{sh,s}$	$\gamma_{sh,\psi}$	$\gamma_{sh,c}$	$\gamma_{sh,a}$
(x)	$t_c=2$	$RH=0.4$	$vs=5.987$	$S=4.5$	$\psi=100$	$c=1075$	$a=7$
$\gamma_{sh,(x)}$	1.15	1.00	1.17	1.08	1.10	1.14	1.01

where,  $t-t_c$  is the time of concrete age after initial curing,  $f$  is a function of volume – to – surface ratio ( $V/S$ ), or  $f=26.0e^{(1.42 \times 0.01(V/S))}$ ;  $\varepsilon_{shu}$  is defined as ultimate shrinkage which is  $780 \gamma_{sh} \times 10^{-6}$  mm/mm (or in./in.). The ACI 209R-92 model suggested using the adjust factor ( $\gamma_{sh}$ ) as below:

$$\gamma_{sh} = \gamma_{sh,tc} \gamma_{sh,RH} \gamma_{sh,vs} \gamma_{sh,s} \gamma_{sh,\psi} \gamma_{sh,c} \gamma_{sh,a} \quad (\text{Eq. 10})$$

Where  $\gamma_{sh,tc}$  is the initial moist curing coefficient;  $\gamma_{sh,RH}$  is the ambient relative humidity coefficient;  $\gamma_{sh,vs}$  is the volume-surface ratio;  $\gamma_{sh,s}$  is the slump factor;  $\gamma_{sh,\psi}$  is the fine aggregate factor;  $\gamma_{sh,c}$  is the cement content factor and  $\gamma_{sh,a}$  is air content factor.

This existing ACI 209R-92 model is similar with the model developed in this paper, since they are all functions of time multiply by an ultimate shrinkage. However, the ACI 209R-92 model does not have adjustment factors for use of SCMs in concrete, and therefore, not suitable for predicting shrinkage of concrete with SCM replacements.

To test the newly-developed model, as expressed in Equation 8, two additional mortar mixes (Mixes 8-pc\* and 9-20FA\*) were made and their autogenous and drying shrinkages were measured with time up to 56 days. The measurements are intended to be compared with the predicted values.

To predict the drying shrinkage of these two new mortars, the ultimate drying shrinkage of a basic mix (Mix8-pc') is firstly determined based on the ACI 209R-92 model according to Equations 8 and 9.

Table 5 shows the factors described in Equation 10. Multiplying those factors,  $\gamma_{sh}=1.84$  is obtained. According to Equation 9, the ultimate free drying shrinkage of the basic mix (without SCM) is:

$$\varepsilon_{sh}(56) = \frac{56}{28+56} \bullet 780 \times 10^{-6} \times 1.84 = 957 \times 10^{-6} \text{ mm/mm}$$

There was only has 4% deferent from the measured free drying shrinkage ( $996 \times 10^{-6}$  mm/mm) of the PC mix. The shrinkage values of those two mixes are presented in Table 6.

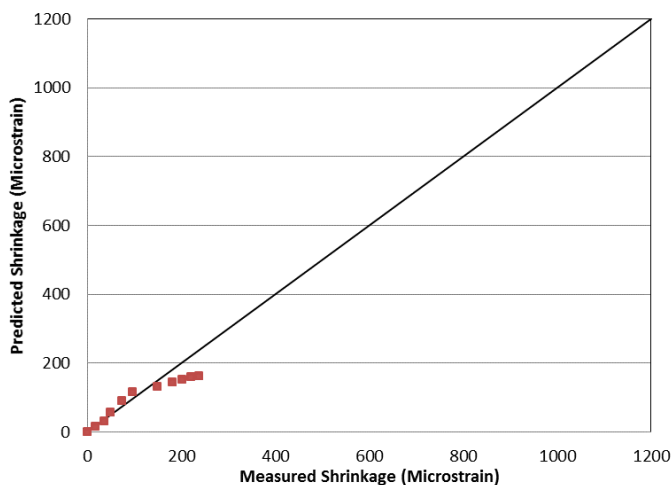


**Table 6** Shrinkage values for Mixes 8 and 9

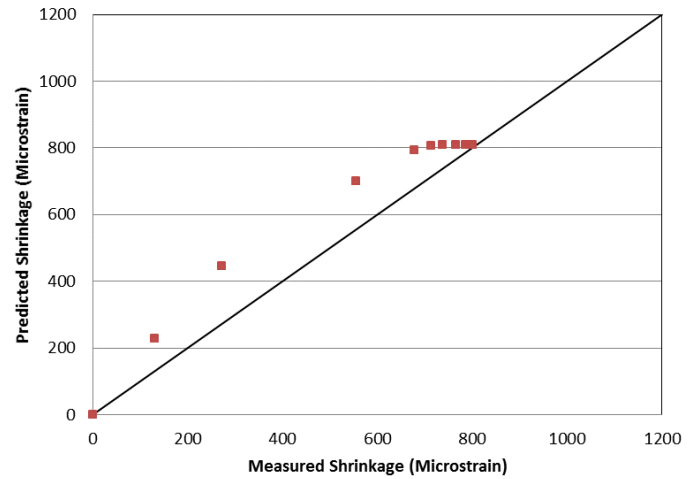
Age (day)	Drying		Autogenous	
	Micro strain (10 <sup>-6</sup> mm/mm)			
	8-PC'	9-20F'	8-PC'	9-20F'
0	0	0	0	0
1	231	131	16	16
3	541	231	49	35
7	793	555	69	49
14	875	677	111	74
21	934	712	136	96
28	954	737	176	148
35	996	765	216	180
42	989	786	233	202
49	985	793	242	220
56	996	800	250	238

Then, other parameters required by Equation 8 are determined, including the normalized ultimate shrinkage (NS), which was 0.85, according to Equation 7, and the growth rates (c), which were -0.28 and -0.05 for drying and autogenous shrinkage, respectively according to Equation 3.

Figure 9 shows the relationship between measured and predicted shrinkages. As seen from Figure 9, the shrinkage data points close to the line  $y = x$ , especially at the ultimate age. This suggests that the model is valid and can well predict shrinkage behavior of concrete and mortar made with materials similar to those used in the present study. The values of the parameters in the model may vary when different concrete materials are used.



(a) Autogenous shrinkage



(b) Drying shrinkage

**Figure 9** Verification of predicted and measured shrinkage values (Mix 9)

It should be noted that the simplified statistical model in this study was developed from the shrinkage data tested in this study only. Therefore, this developed model may not be appropriately used to predict the shrinkage of the mortar which having different conditions from this study; such as, different types of fly ash and GGBFS, different specimen sizes, different environment condition, different paste content, different maximum aggregate sizes and etc.

## 6. Conclusion

In this paper, an experimental investigation is conducted to study the effects of GGBFS and class C fly ash (FA) on autogenous shrinkage and drying shrinkage of HPC mortar. A statistic model was developed and tested based on the experimental data. The following conclusions can be made based on the obtained results:

- (1) FA replacement reduced both autogenous shrinkage and drying shrinkage of mortar; therefore, it reduced the total shrinkage of HPC. GGBFS replacement increased the autogenous shrinkage, but reduced the drying shrinkage.
- (2) The exponential model,  $\varepsilon(t) = a + b \cdot e^{(c \cdot t)}$ , can well describe both autogenous and free drying shrinkage (at any age of  $t$ ) of concrete mortar containing GGBFS or fly ash with R-squares of 0.95 or higher.
- (3) Using a term of normalized ultimate shrinkage, defined as  $NS = \frac{\varepsilon_{ult,scm}}{\varepsilon_{ult,control}}$ , the shrinkage prediction model can be simplified as  $\varepsilon_{scm}(t) = NS \cdot \varepsilon_{ult,control} \cdot [1 - 0.95e^{(c \cdot t)}]$ . Using this prediction model, the autogenous or drying shrinkage of mortar or concrete with a SCM (GGBFS or fly ash) at any testing age can

be predicted as long as the ultimate autogenous or ultimate drying shrinkage of mortar or concrete without SCM is known (either calculated from the ACI 209R-92 model or measured).

- (4) Test results from additional mortar mixes suggests that the newly developed statistical model can well predict shrinkage behavior of concrete and mortar made with materials similar to those used in the present study.

## 7. Acknowledgement

The authors sincerely thank Dr. Chen Yu, Changsha University of Science & Technology, China, for her advices on the present research during her visit at Iowa State University. The supply of concrete materials from Iowa Department of Transportation, USA, is also greatly acknowledged.

## 8. References

- [1] Y. Li, J.Bao and Y. Guo, "The relationship between autogenous shrinkage and pore structure of cement paste with mineral admixtures", *Construction and Building Materials*, Vol.24, pp.1855-1860, 2010.
- [2] V. M. Sounthararajan and A.Sivakumar, "Drying Shrinkage Properties of Accelerated Fly Ash Cement Concrete Reinforced with Hooked Steel Fiber", *ARPN Journal of Engineering and Applied Sciences*, Vol. 8, No. 1, pp. 77-85, 2013.
- [3] Z. Jiang, Z. Sun and P. Wang, "Autogenous relative humidity change and autogenous shrinkage of high-performance cement pastes", *Cement and Concrete Research*, Vol.35, pp.1539-1545, 2005.
- [4] J.Li, and Y.Yao, "A study on creep and drying shrinkage of high performance concrete," *Cement and Concrete Research*, vol. 31, no. 8, pp. 1203-1206, 2001.
- [5] W. Hansen, "Constitutive Model for Predicting Ultimate Drying Shrinkage of Concrete", *J. Am. Ceram. Society*, vol. 70, no. 5, pp. 329-32, 1987.
- [6] *Guide for Modeling and Calculating Shrinkage and Creep in Hardened Concrete*, ACI 209.2R-08, 2008.
- [7] *Standard Test method for Autogenous Strain of Cement Paste and Mortar*, ASTM C1698-09, 2010.
- [8] *Standard Test Method for Drying Shrinkage of Mortar Containing Hydraulic Cement*, ASTM C596-09, 2010.
- [9] ACI Committee 226, "Ground Granulated Blast-Furnace Slag as a Cementitious Constituent in Concrete," American Concrete Institute, ACI 226.1R-87, *ACI Materials Journal*, Vol. 84, No. 4, p.327-342, 1987.
- [10] S.Tangtermsirikul, "Class C Fly Ash as a Shrinkage Reducer for Cement Paste," *ACI Special Publication*, American Concrete Institute, Volume 153, pp. 385-402, 1995.
- [11] L. H. Jiang and V. M Malhotra, "Reduction in Water Demand of Non-air-entrained concrete Incorporating Large Volumes of Fly Ash", *Cement and Concrete Research*, Vol. 30, No. 11, pp. 1785-1789, 2000.
- [12] Holt, E. E., "Early Age Autogenous Shrinkage of Concrete", *VTT Building and Transport*, Technical Research Center of Finland, ESPOO, 2001.
- [13] S. Kawashima and S. P. Shah, "Early-age autogenous and drying shrinkage behavior of cellulose fiber-reinforced cementitious materials," *Cement and Concrete Composites*, vol. 33 pp. 201-208, 2011.
- [14] JMP®, Version <11>.SAS Institute Inc., Cary, NC, 1989-2014.